Thermodynamic exploration of temperature vacuum swing adsorption for direct air capture of carbon dioxide in buildings

Ruikai Zhao[a,*], Longcheng Liu[a], Li Zhao[b,c], Shuai Deng[b,c,*], Shuangjun Li[b,c], Yue Zhang[b,c], Hailong Li[d]

[a] Department of Chemical Engineering, KTH Royal Institute of Technology, SE-100 44 Stockholm, Sweden
[b] Key Laboratory of Efficient Utilization of Low and Medium Grade Energy (Tianjin University), Ministry of Education of China, Tianjin 300350, China
[c] International Cooperation Research Centre of Carbon Capture in Ultra-Low Energy-Consumption, Tianjin 300350, China
[d] School of Business, Society and Engineering, Mälardalen University, SE-721 23 Västerås, Sweden

ABSTRACT

Abrupt climate change such as the loss of Arctic sea-ice area urgently needs negative emissions technologies. The potential application of direct air capture of carbon dioxide from indoor air and outdoor air in closed buildings or crowded places has been discussed in this paper. From the aspects of carbon reduction and indoor comfort, the ventilation system integrating a capture device is of great value in practical use. For ultra-dilute carbon dioxide sources, many traditional separation processes have no cost advantages, but adsorption technologies such as temperature vacuum swing adsorption is one of suitable methods. Thermodynamic exploration has been investigated regarding minimum separation work and second-law efficiency at various concentrations in the air. The influence of concentration, adsorption temperature, desorption temperature and desorption pressure on the energy efficiency has also been evaluated. Results show that the minimum separation work for the level of 400 ppm is approximately 20 kJ/mol. The optimal second-law efficiencies are 44.57%, 37.55% and 31.60%, respectively for 3000 ppm, 2000 ppm and 1000 ppm. It means that a high energy-efficiency capture device in buildings merits attention in the exploration of the possibility of approaching negative carbon buildings.

1. Introduction

In recent decades, Arctic sea ice has declined rapidly with the rise of global temperatures, atmospheric carbon dioxide concentrations and cumulative carbon emissions [1]. The Paris Agreement about climate change achieves a goal of '*holding the increase in the global average temperature to well below 2 °C*' and '*to pursue efforts to limit the temperature increase to 1.5 °C*' [2]. However, the latest study has revealed that global average temperature to limit warming to 1.5 °C rather than 2.0 °C has the potential to prevent a loss of multiyear sea ice in the Arctic [3]. Facing serious Arctic sea-ice loss and other threats arising from climate change, most scenarios need negative emissions technologies (NETs), in order to meet the requirement of the Paris Agreement [4]. The reason is that carbon dioxide (CO_2) emissions cannot be reduced rapidly enough to keep the total stock sufficiently small to limit the temperature increment successfully.

Deployment and research of so-called NETs, for example, bioenergy with carbon capture and storage (BECCS) [5], and direct air capture of CO_2 from ambient air and storage (DACS) [6], etc., could reduce the carbon stock in the atmosphere significantly. Table 1 presents a summary of technical classification for ten typical NETs [7] from the methods of capture and storage. The advantage of DACS is that systems can be decoupled in space and time from the exiting power plants and be situated in the strategy level next to a renewable energy source and/or a final storage place [8].

The CO_2 capture technologies, such as absorption, adsorption and membrane, etc., have received widespread attention in recent years. Li et al. [9] have performed a report on patented innovations on carbon dioxide capture technology. Mondal et al. [10] have provided a literature review on the existing and emerging technologies for CO_2 capture. However, these technologies have focused on carbon dioxide capture from the exhaust gas, which is emitted from the power plants. Aiming at reducing CO_2 concentrations back to the pre-industrial levels should require its capture not only from large emission sources such as flue gas but also point sources such as living spaces [11]. However, CO_2 capture from dilute ambient air at point sources requires high energy

Nomenclature

Acronyms

BECCS	bioenergy with carbon capture and storage
DAC	direct air capture
DACS	direct air capture of CO_2 from ambient air and storage
NETs	negative emissions technologies
PSA	pressure swing adsorption
TSA	temperature swing adsorption
TVSA	temperature vacuum swing adsorption
VSA	vacuum swing adsorption

Greek letters

η	efficiency (%)

Subscripts

ac	actual
ads	adsorption
des	desorption
H	high temperature
L	low temperature
pump	vacuum pump
s	solids

Symbol

C_p	specific heat (J/kg K)
$\triangle H$	heat of adsorption (kJ/mol)
LW	lost work (kJ/mol)
m	mass (g)
P	pressure (Pa)
Pu	purity (%)
Q	heat (kJ/mol)
q	the amount of CO_2 adsorption (mol/kg)
Re	capture rate (%)
T	temperature (K)
W	work (kJ/mol)
WC	working capacity (mol/kg)
x	concentration (%)

consumption, which is 3 to 4 times the energy for carbon dioxide capture from exhaust gases [12]. Hence, an energy-efficient approach of direct air capture (DAC) is necessary for achieving stringent climate targets.

Actually, the basic principle of DAC technologies, such as absorption, adsorption and membrane, make no significant difference in those applied to capture carbon dioxide from flue gas, apart from the requirement of materials and energy consumption. Firstly, to develop a viable composite sorbent, Ounoughene et al. [13] have studied the carbon capture performance of an ethanol/calcium oxide mixture which is exposed to the ambient air. Secondly, as an extension of adsorption, for example, the diamine-functionalized silica gel has been experimentally analyzed for carbon capture from dry and humid atmospheric air [8]. Recently, Wang et al. [14] have revealed the characterisics of the resin-based sorbent for air capture via moisture swing adsorption. At last, some membrane separation technologies used for the flue gas also have been extended to DAC, for instance, a unit of bipolar membrane electrodialysis has been experimentally investigated

Table 1
Technical classification of ten ways of typical NETs.

NETs		Capture		Storage	
		Biological	Non-biological	Biological	Geological
1	DACS		√	√	√
2	BECCS	√			√
3	Cloud treatment to increase alkalinity		√	√	
4	Enhanced ocean productivity	√		√	
5	Enhance weathering		√	√	
6	'Blue carbon' habitat restoration	√		√	
7	Afforestation and reforestation	√		√	
8	Building with biomass	√		√	
9	Biochar	√			√
10	Soil carbon sequestration	√			√

Note: Biological capture is by photosynthesis; biological storage is in the biosphere whose carbon stock increases; geological storage is in the deep below ground.

for atmospheric carbon dioxide separation with caustic solvents [15]. Furthermore, there are some reviews and cyclic analysis for direct air capture. For example, Sanz-Pérez et al. [16] have reviewed the advances made in the field of DAC. More recently, Elfving et al. [17] have studied the equilibrium working capacity of various processes, including pressure swing adsorption (PSA) and temperature swing adsorption (TSA), for CO_2 separation under DAC conditions. Although such considerable application efforts provide several methods for CO_2 separation from ambient air, there are a handful of studies on exploring the possibility of the small-scale applications such as building environment.

The CO_2 concentration in living spaces, such as closed buildings and crowded places, is usually higher than that of the atmospheric air [18]. However, some standards indicate that the maximum acceptable indoor CO_2 level is typically below 1000 ppm [19]. Too high values of CO_2 level in the air could increase partial blood pressure, which results in breathing difficulties and increased frequency of breaths [20]. Guidelines of ventilation call for indoor CO_2, as an indicator for indoor air quality, not to exceed 700 ppm above outdoor levels [21]. For the sake of improving the indoor air quality and reducing CO_2 concentration in crowded spaces, several studies on the CO_2 level of building environment which is between those of ambient air and flue gas have been undertaken recently, and most of them are CO_2 adsorption technologies. For instance, Gall et al. [22] have evaluated four low-cost Ca- and Mg-based sorbents for potential use in indoor air cleaning applications in three types of indoor environments. A comparative study of energy savings about fan power between integrating a CO_2 capture device into an air supply unit and a conventional ventilation system has been investigated by Kim et al. [23]. Lee et al. [24] have discussed the influence of the operation variables on the electrical energy requirement and efficiency of electric-swing adsorption for CO_2 removal from living spaces. Han et al. [25] have conducted a performance testing of a PSA system for efficient O_2 supply to room air supply unit combined with carbon dioxide adsorption device. Hu et al. [26] have studied the impacts of design parameters, including removal efficiency and pressure drop, on the performance of the modified activated carbon filter for CO_2 capture. Nonetheless, there is no research has conducted an energy efficiency analysis via a thermodynamic model for DAC in buildings.

From both views of improving indoor air quality and reducing carbon emission, incorporating a DAC device into buildings is of great value in practical use. However, CO_2 capture technologies are excluded

in the present studies of zero-energy or zero-carbon buildings. For instance, Xing et al. [27] have reviewed a range of advanced technologies for zero carbon refurbishment, such as building fabrics, high energy efficient building devices and renewable technologies, and carbon capture techniques were not included. The same exclusion has occurred in literature research on performance evaluation of net zero-energy building presented by Deng et al. [28]. Therefore, if possible, a high energy-efficiency CO_2 capture technology would have an outstanding performance in the field of building energy conservation.

A combination of TSA and vacuum swing adsorption (VSA), which is known as temperature vacuum swing adsorption (TVSA), can reduce the time of CO_2 desorption significantly compared to the means of TSA or VSA [29]. Plaza et al. [30] have found that the productivity and purity of desorbed CO_2 with activated carbon followed the order TVSA > VSA > TSA. Hence, the cyclic operation of TVSA with a promising adsorbent material would be energy efficient with a high product purity and productivity.

In this study, a capture device, which utilizes a TVSA cycle, is innovatively integrated into the ventilation system of buildings for capturing CO_2 from indoor air and outdoor air. The novelty of this paper, therefore, aims to conduct an energy-efficiency analysis of TVSA for capturing CO_2 under various conditions in the building section. A thermodynamic model of TVSA for DAC is presented in Section 2. The influence of different parameters, such as CO_2 level, desorption temperature (T_{des}), adsorption temperature (T_{ads}) and desorption pressure (P_{des}), on the second-law efficiency of TVSA is discussed in Section 3. Section 4 provides a further exploration for approaching negative carbon buildings. Finally, the conclusion and future work are given in Section 5.

2. Direct air capture of carbon dioxide in buildings

A simplified diagram of a building with the air ventilation system incorporating a carbon dioxide adsorption device is illustrated in Fig. 1. A hypothetical room is conceived for 15 occupants with dimensions of 10 m (W) × 10 m (L) × 3.0 m (H). The indoor CO_2 concentration is increased during the office hours from 9:00 am to 5:00 pm, due to the breathing of the occupants. The breathing zone in the office room is assumed to be well mixed, and the room temperature is controlled and maintained at 298 K by air-conditioning. Furthermore, the CO_2 level of the outdoor air is assumed to be 400 ppm, and CO_2 level of the indoor air is higher than 400 ppm due to occupants' breathing.

2.1. Process description

The inlet and outlet ventilating ducts for the circulation between the indoor and outdoor air are wall-mounted, as demonstrated in Fig. 1. When the valves of V1 and V2 are open, the outdoor and indoor air can be exchanged by air blowers. In order to capture CO_2 from indoor air and outdoor air, a CO_2 capture device packed with adsorbent materials is constructed in parallel with the ventilating pipes, as shown in Fig. 1. The application of TVSA cycles for DAC increases the implementation challenges and control complexity in buildings.

When some valves (V1, V2, V5 and V6) are closed and the other valves are open, the air circulation will go through the capture device by fans and CO_2 would be captured by the adsorbents in the adsorption chamber. At the step of regeneration, the adsorbents with the adsorbed CO_2 are heat by thermal medium or Joule effect of the current. Then, CO_2 is desorbed and transported to the gas cylinder via vacuum pump, as the valves of V3 and V4 are closed. Finally, the adsorption chamber is cooled by the outdoor air or indoor air, according to valve transformation. As the temperature of the chamber is down to the suitable temperature for CO_2 capture, a new cycle starts. The stored CO_2 in the cylinder can be used to the gas fertilizer or fuel synthesis.

2.2. Adsorbent material

The adsorbent material studied in this paper is amine-functionalized cellulose, which is applied in a direct air capture device as a kind of chemosorbent. Material properties of this adsorbent such as adsorption isotherm were studied previously and sourced from Ref. [31]. Usually, the adsorption capacities of the adsorbent material are determined by temperature and CO_2 partial pressure. A Toth-type isotherm, Eq. (1), is used to simulate the adsorption capacity of adsorbents, as it properly represents the majority of adsorbents in the practical separation processes.

$$q = \frac{n_s b P_{CO2}}{(1 + (b P_{CO2})^t)^{\frac{1}{t}}} \tag{1}$$

where q is the adsorption capacity; P_{CO2} is the CO_2 partial pressure; n_s, b and t are parameters of Toth model. Specifically, n_s represents the maximum adsorption capacity; b is the adsorption affinity; t refers to the system heterogeneity. These parameters of Eq. (1) are temperature-dependent and can be shown as follows:

$$n_s = n_0 e^{a\left(1 - \frac{T}{T_0}\right)} \tag{2}$$

$$b = b_0 e^{\frac{\Delta H_0}{R T_0}\left(\frac{T_0}{T} - 1\right)} \tag{3}$$

$$t = t_0 + c\left(1 - \frac{T_0}{T}\right) \tag{4}$$

where n_0 and b_0 are values of these parameters at a reference temperature of T_0; a, c and t_0 are dimensionless constants; R is the ideal gas constant; The parameter of ΔH_0 is the opposite number of the heat of adsorption, which is set as 60 kJ/mol in this model. Table 2 lists the above parameters of Toth model for the used adsorbent [32]. Fig. 2 illustrates the contours plot of CO_2 adsorption capacity in the plane of pressure and temperature. As expected, the CO_2 adsorption capacity always increases with the partial pressure but decreases with temperature. Hence, the values of q at the top-left corner are less than that of bottom right corner.

2.3. Thermodynamic model

Fig. 2 also presents qualitatively an idealized TVSA cycle for CO_2 capture under equilibrium conditions in the chart of adsorption isotherm. The cycle description of TVSA processes is conducted on the basis of several assumptions [33]: (1) Uniform temperature in the adsorbent materials is supposed; (2) Uniform CO_2 concentration in the adsorbent materials is also supposed at the equilibrium state [34]; (3) Other components in the ambient air such as N_2 and O_2 are not considered and are supposed to be an inert gas for simplicity [35].
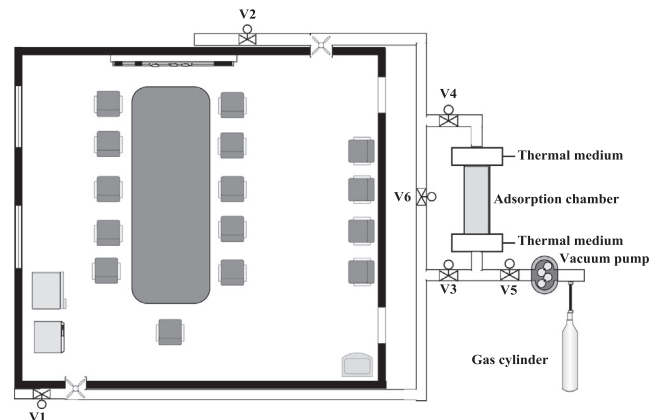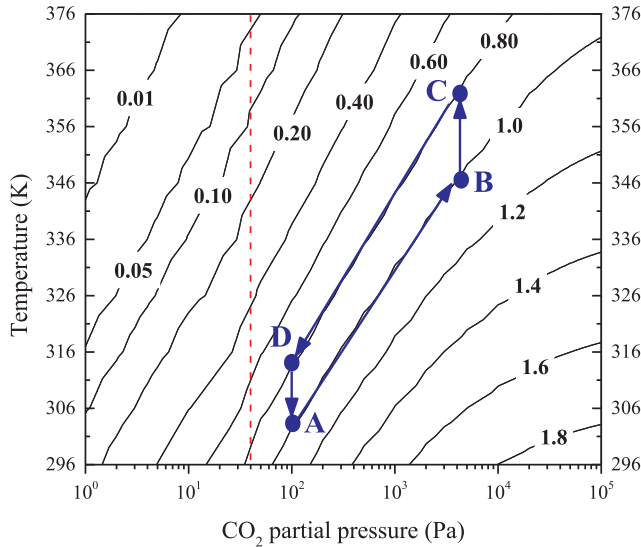

Fig. 1. Schematic diagram of an air ventilation system incorporating a CO_2 capture device.

Table 2
The parameters of the Toth model for the used adsorbent.

Parameter	Value
T_0 (K)	296
b_0 (1/mbar)	22.50
n_0 (mol/kg)	1.97
ΔH_0 (kJ/mol)	60
R (J/mol K)	8.314
t_0	0.422
a	2.37
c	0.949

Fig. 2. The contours of CO_2 adsorption capacity [mol/kg] as a function of pressure and temperature. The parallelogram ABCD indicates the each step of a TVSA cycle. The dashed line depicts CO_2 partial pressure of outdoor air (40 Pa).

In the adsorption process of TVSA shown here, point A depicts the equilibrium state after adsorbents have been saturated with the indoor air at adsorption temperature (i.e. 298 K in Fig. 2) and CO_2 partial pressure (i.e. 100 Pa in Fig. 2). The corresponding equilibrium CO_2 loading of the adsorbent at point A is q_{max}, i.e. 1.0 mol/kg in Fig. 2. Actually for the adsorption process, the CO_2 adsorption amount of the adsorbents rises to point A from a low value that is q_{min}, i.e. 0.8 mol/kg in Fig. 2.

The desorption process (A → B → C) begins with a vacuum pump evacuating the adsorption chamber to the desired CO_2 partial pressure (i.e. 4000 Pa in Fig. 2). At the same time, the temperature of the adsorbent is increased from T_A (i.e. 298 K in Fig. 2) to T_B (i.e. 346 K in Fig. 2), for the first section of the heating process (A → B). There is no CO_2 which is released into the volume around the adsorbent material at this phase, as indicated by points A and B. Subsequently, carbon dioxide is continually desorbed and removed by a vacuum pump until the desorption temperature of adsorbent materials reaches T_C (i.e. 363 K in Fig. 2), for the second stage of the heating process. The corresponding equilibrium CO_2 loading of the adsorbent material declines from 1.0 mol/kg to 0.8 mol/kg, indicated by points B and C.

During the cooling process (C → D → A), the adsorbent material is exposed to a gas stream (i.e. the indoor ambient air) with the room temperature (i.e. 298 K in Fig. 2) and CO_2 partial pressure (i.e. 100 Pa in Fig. 2). The temperature of the adsorbent material decreases from T_C to T_A, and no CO_2 is deemed to desorb at this step due to the increasing adsorption capacity (the CO_2 adsorption amount is q_{min} at this step). The next cycle is restarted until T_A is reached.

For a TVSA cycle, the significant performance criterion is the CO_2

working capacity (WC_{TVSA}), which can be defined in Eq. (5) as follow:

$$WC_{TVSA} = q_{max} - q_{min} \qquad (5)$$

where q_{max} is the maximum equilibrium CO_2 loading in the TVSA cycle; q_{min} is the minimum equilibrium CO_2 adsorption amount in the TVSA cycle.

As described in the previous section, the energy consumption for the adsorbent regeneration in the TVSA cycle is given by the heat input (Q_H) for taking the adsorbents to the required desorption temperature (T_{des}) from the adsorption temperature (T_{ads}) and the CO_2 desorption enthalpy ($\Delta H(q)$), and the work input (W_{pump}) for running the vacuum pump to the required desorption pressure (P_{des}). It is assumed that the heat input for the product gas stream is negligible due to its small scale. The equations of the heat input (Q_H) and the work input (W_{pump}) are shown as follows:

$$
\begin{aligned}
Q_H &= \frac{m_{solids}C_{p,s}(T_{des} - T_{ads}) + m_{solids}\int_{q_{min}}^{q_{max}} \Delta H(q)dq}{m_{solids}WC_{TVSA}} \\
&= \frac{C_{p,s}(T_{des} - T_{ads}) + \int_{q_{min}}^{q_{max}} \Delta H(q)dq}{q_{max} - q_{min}}
\end{aligned} \qquad (6)
$$

$$W_{pump} = \frac{1}{\eta_{pump}}RT_{des}\ln\left(\frac{P_{ads}}{P_{des}}\right) \qquad (7)$$

where m_{solids} is the mass of the adsorbent material at the adsorption chamber; $C_{p,s}$ is the heat capacity of the adsorbent material and is assumed to be 900 J/kg K in this study; η_{pump} is the efficiency of vacuum pump with respect to isothermal compression at the required desorption temperature (T_{des}) and is supposed to be 0.70; P_{ads} is the adsorption pressure, i.e. 1.0 bar in this paper; P_{des} is the desorption pressure, i.e. 0.1 bar; $\Delta H(q)$ is the CO_2 desorption enthalpy and is fitted from the test results [31] as a function of CO_2 adsorption amount indicated in Eq. (8).

$$\Delta H(q) = 65.26 - 17.74 \times q \qquad (8)$$

The separation process of TVSA is established using a feed gas stream with different composition of CO_2 at the temperature of 298 K and the pressure of 1.0 bar for all processes studied, as shown in Fig. 3. Fig. 3 presents the mole balances and energy balances for the separation process of TVSA. The separation process has a feed gas stream, a waste gas stream and a product gas stream. The component of CO_2 in the feed gas is labeled A, and the inert gas is labeled B. The main objective of this study is to investigate the separation efficiency (i.e. the second-law efficiency) of a TVSA cycle. However, the factors including chamber pressure drop, bed geometric dimensioning, mass transfer and other dynamic effects, are not considered in this analysis. Usually, the separation process is supposed to capture 90% of carbon dioxide in the
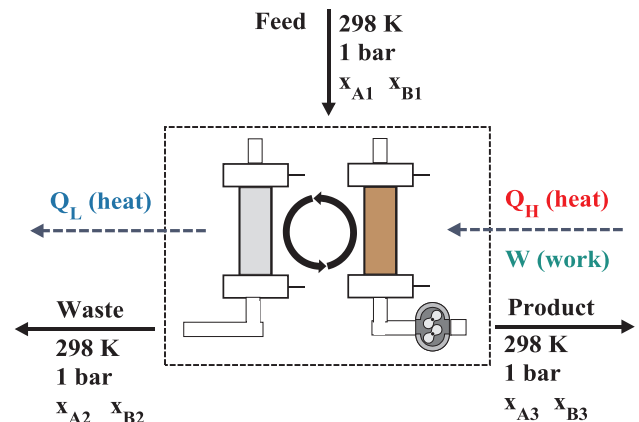
Fig. 3. The ideal binary separation system for a TVSA cycle. The dashed box around the processes depicts the system boundary.

incoming gas, and the purity of the product gas stream ($x_{A,3}$) at 298 K and 1.0 bar is specified to be 95%. Based on the above assumptions, the flows and mole fractions is applied to calculate the minimum separation work (W_{min}), i.e. the free energy of mixing [12], as given in Eq. (9). The input gas is regarded as mixtures of ideal gases. W_{min} is the theoretical minimum to completely separate the input gas into two flows. The evolution of this formulas can be found in the study of Zhao et al. [36]. In this analysis, W_{min} mainly depends on four parameters including the CO_2 concentration in the feed gas ($x_{A,1}$), separation temperature (T_{ads}), and CO_2 recovery (Re_{CO2}) and product purity (Pu_{CO2}).

$$W_{min} = \Delta G = \frac{RT}{n_3 x_{A,3}}[n_3(x_{A,3}\ln x_{A,3} + x_{B,3}\ln x_{B,3})$$
$$+ n_2(x_{A,2}\ln x_{A,2} + x_{B,2}\ln x_{B,2}) - n_1(x_{A,1}\ln x_{A,1} + x_{B,1}\ln x_{B,1})] \qquad (9)$$

The second-law efficiency of TVSA (η_{TVSA}) in the practical processes is defined as the ratio of the minimum separation work to the actual work (W_{ac}) [37], as shown in the following equation. The actual work includes W_{min} and lost work (LW_{TVSA}). LW_{TVSA} is essentially work wasted as a result of irreversibility in the practical processes. As for the TVSA cycle, the actual work includes the power consumption of the pump and the available energy of the total input heat as well.

$$\eta_{TVSA} = \frac{W_{min}}{W_{ac}} = \frac{W_{min}}{W_{min} + LW_{TVSA}} = \frac{W_{min}}{W_{pump} + Q_H\left(1 - \frac{T_0}{T_H}\right) - Q_L\left(1 - \frac{T_0}{T_L}\right)} \qquad (10)$$

The temperature of heat source (T_H) is equal to the desorption temperature (T_{des}). Q_L stands for the heat for adsorbent cooling and Q_H is the input heat per cycle. The low temperature for cooling (T_L) is supposed to be the ambient temperature according to the above cycle description. The reference (or ambient) temperature (T_0) is set as 298 K in this analysis [38].

3. Results and discussion

In order to maintain appropriate air quality, CO_2 levels should be designed to keep below 1000 ppm. There is a study that 3000 ppm is selected as the unacceptable level for CO_2 capture from the living spaces [24]. Thus, the cases of CO_2 levels at 400 ppm, 700 ppm, 1000 ppm, 2000 ppm and 3000 ppm are evaluated from the aspects of W_{min}, T_{ads}, T_{des} and P_{des}. The thermodynamic analysis of the TVSA cycle for DAC reveals the relationship between the second-law efficiency and

CO_2 concentrations.

3.1. Minimum separation work

The physical significance of the minimum separation work is an evaluation indicator for the difficulty grade of the CO_2 separation process. Substantially, the large value of W_{min} would lead to the difficulty of separation treatment. Fig. 4 shows the strong positive effects of CO_2 recovery, separation temperature and product purity on the value of W_{min}. More specifically, the minimum separation work increases with the rising of CO_2 recovery. For example, W_{min} increases from 17.91 kJ/mol to 19.33 kJ/mol, as CO_2 recovery is from 30% to 90% for CO_2 concentration of 700 ppm. It is clearly shown that the higher product purity requires the large value of W_{min} for a CO_2 level of 400 ppm, such as the changes of P_u from 95% to 99%. The rising trend of W_{min} at CO_2 recovery of 90% is observed with the increase of separation temperature: at T = 298 K, 308 K and 318 K, W_{min} increases to 15.72 kJ/mol, 16.25 kJ/mol and 16.78 kJ/mol, respectively. Fig. 4 also demonstrates the adverse impact of CO_2 level in the feed gas on W_{min}. For instance, a separation process with separation temperature of 298 K, CO_2 recovery of 90% and product purity of 95%, W_{min} of CO_2 level at 400 ppm is 20.72 kJ/mol, which is 2.28 kJ/mol larger than W_{min} of CO_2 level at 1000 ppm, and is more than 1.3 times larger than the corresponding value for 3000 ppm. It's worth noting that W_{min} of CO_2 level at 400 ppm is approximately 20 kJ/mol, and these results are trustworthy according to the study of the free energy of mixing [39].

3.2. Analysis of second-law efficiency

The second-law efficiency is mainly applied to evaluate the separation efficiency of the TVSA cycle for DAC. Generally, the separation requirement for CO_2 capture is that the recovery rate is 90% and the product purity is 95%, which is conducted as an assumption of the following analysis. Therefore, the energy-efficiency performance of TVSA is estimated through a parametric study from the view of circulation. For the later study, desorption temperature is set as 373 K and adsorption temperature is set as 298 K, except where noted in this section.

3.2.1. Desorption temperature

Desorption temperature has the positive influence on the CO_2 working capacity per cycle, as shown in Fig. 2. Considering the

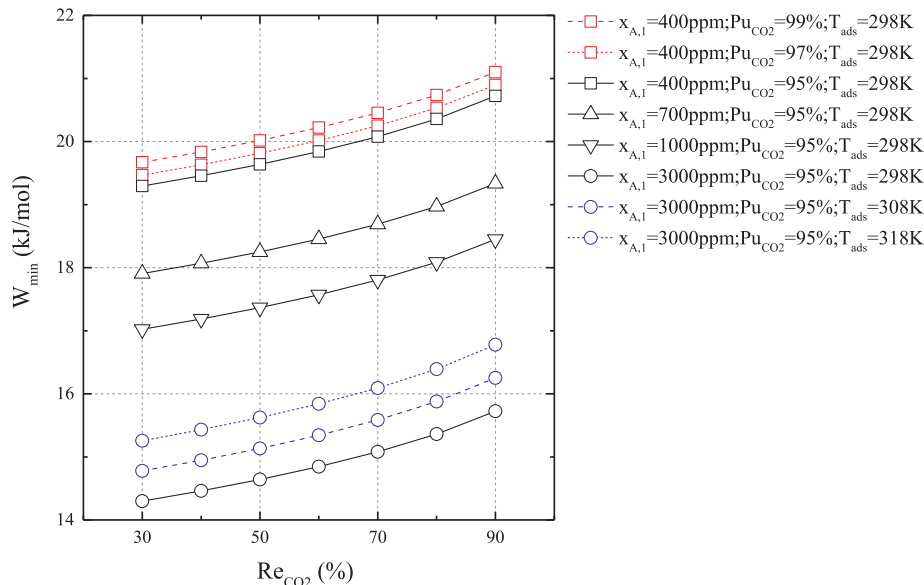**Fig. 4.** The minimum separation work of DAC as a function of CO_2 recovery, CO_2 level in the feed gas, separation temperature and product purity.

application of TVSA in the air ventilation system of the building for DAC, desorption temperature cannot be too high because of fire danger. Therefore, the variation of desorption temperature is controlled in the range of 333–403 K.

As shown in Fig. 5, there are thermodynamically optimal second-law efficiencies concerning desorption temperatures for various CO_2 concentrations of the feed gas. Specifically, the optimal second-law efficiencies are 44.57%, 37.55% and 31.60%, respectively for 3000 ppm, 2000 ppm and 1000 ppm. Correspondingly, the optimal desorption temperatures decline as CO_2 levels grow from 1000 ppm to 3000 ppm. The results show that the cases which deal with the high CO_2 levels in the feed gas are more efficient. The underlying cause is that the CO_2 working capacity decreases with the increase of CO_2 levels, which leads to the increase of the heat input. It is important to note that the second-law efficiencies of several special cases are zero because the corresponding working capacities are zero at the special low desorption temperatures. For example, the desorption temperatures that the corresponding second-law efficiencies are zero are 336 K, 348.5 K, 356 K and 368 K, respectively for 2000 ppm, 1000 ppm, 700 ppm and 400 ppm. In essence, the minimum separation work of various CO_2 levels is unchanged when desorption temperatures are increased. Thus, the dominant factor that affects the second-law efficiency is the heat input with the variation of desorption temperatures.

3.2.2. Adsorption temperature

From the Fig. 2, it can be found that the adsorption temperature has an adverse impact on the CO_2 working capacity per cycle. Because the input heat is released into ambient air by the cooling method of the adsorption chamber, the adsorption temperature for CO_2 capture may increase after a series of cycles. Consequently, the change of adsorption temperature could be set within a range of 298–323 K.

Fig. 6 illustrates the downtrend of the second-law efficiency with the rise of adsorption temperature for different CO_2 levels. For instance, the second-law efficiency of CO_2 level at 3000 ppm declines from 39.41% to 15.38% as adsorption temperature grows from 298 K to 323 K. The results present that the cases of the high CO_2 levels in the feed gas are more efficient compared to that of lower concentrations. More specifically, the cases of CO_2 level at 3000 ppm is the highest rank in the second-law efficiency at this variation of adsorption temperature, followed by 2000 ppm, 1000 ppm, 700 ppm and 400 ppm. The fundamental cause is that the increase of CO_2 concentration results in the decline of CO_2 working capacity, which leads to the increase of the input heat. It appears clearly that the second-law efficiencies of several cases are zero on account of CO_2 working capacity that is zero at the particular adsorption temperature. For example, the adsorption temperatures that the second-law efficiency is zero are 301.3 K, 308.9 K and 313.7 K, respectively for the cases of 400 ppm, 700 ppm and 1000 ppm. It is important to note that the minimum separation work increases with the rise of adsorption temperature (see Fig. 4). However, the decrease of CO_2 working capacity is the main element for the downtrends of the second-law efficiency for these different CO_2 concentrations.

3.2.3. Desorption pressure

Desorption pressure has a negative influence on the carbon dioxide working capacity of TVSA (see Fig. 2 and Eq. (5)). Considering the attainable ultimate vacuum of the existing pumps, the variation of desorption pressure is controlled in the range of 0.05–0.90 bar in this section.

Flat decreases of the second-law efficiency for different CO_2 concentrations (except for 400 ppm) can be observed with the rise of desorption pressure in Fig. 7. Flattening of the second-law efficiency is observed at higher CO_2 levels, especially for 3000 ppm at high desorption pressures. For example, the second-law efficiency of the cases of CO_2 levels at 1000 ppm decreases from 36.00% to 12.97% when desorption pressure rises from 0.05 bar to 0.9 bar. This is due to the increase of desorption pressure that leads to the decrease of the work

input for the pump operating. It is visible that the cases of the high CO_2 level in the feed gas are more efficient than these low concentration's counterparts. Similarly, the largest second-law efficiency at this variation is the cases of CO_2 levels at 3000 ppm, followed by 2000 ppm, 1000 ppm, 700 ppm and 400 ppm. The basic cause is that the increase of CO_2 concentration results in the decease of CO_2 working capacity, which leads to the rise of second-law efficiency. It is also found that there is a zero point as the desorption pressure is 0.17 bar for the cases of CO_2 levels at 400 ppm. This is because the CO_2 working capacity at the corresponding conditions is zero. As given in Fig. 4, there is no impact of desorption pressure on the minimum separation work, which means that the minimum separation work in these cases is constant. Thus, the reducing of the work input for pump running is the main cause for the downtrends of the second-law efficiency for these cases.

In this study, the second-law efficiency is used to evaluate the realistic implementations of a TVSA cycle. Compared to the study of Lackner [39], the second-law efficiency is significantly lower than the theoretical efficiency of the ideal single sorbent process, which defines a theoretical limit just like Carnot efficiencies for heat engines represent an optimum. After all, the actual implementation processes likely perform worse compared to the ideal processes. Nonetheless, the second-law efficiency also offers an optimum for the practical TVSA processes. Specifically, the optimal efficiencies range from 31.60% to 44.57% for 1000–3000 ppm.

Based on the above analysis, it can be found that the minimum separation work for 400 ppm is fairly high. In fact, a flue gas scrubber that capturing CO_2 from flue gas with a concentration of 15% and a capture rate of 90%, has $W_{min} = 6.81$ kJ/mol [36]. Therefore, the amount of energy consumed in the DAC device is about 3 times as large as the energy consumed in a flue gas scrubber. It means that the TVSA cycle is intensive energy-consumed for DAC. For example, the power consumption of the pump is 5.27 kJ/mol and the total input heat is 361.95 kJ/mol ($x_{A,1} = 400$ ppm, $T_{de} = 393$ K and $\eta_{TVSA} = 22.75\%$).

According to the efficiency study, it provides an optimum operating condition for the TVSA cycle, from the point of energy utilization and management. The relationship between the operation conditions and the second-law efficiencies has also been found in these results. For example, the second-law efficiencies of TVSA show a downward trend after the first rise, as the desorption temperature increases. It means that there is an optimum desorption temperature for the running of a TVSA cycle. Therefore, TVSA processes enable high energy-efficiency for DAC, although it is energy-intensive.

Zero carbon buildings (carbon-neutral buildings) are regarded as a solution to solve problems of energy saving, environmental conservation, and carbon emissions reduction in the area of buildings. The main
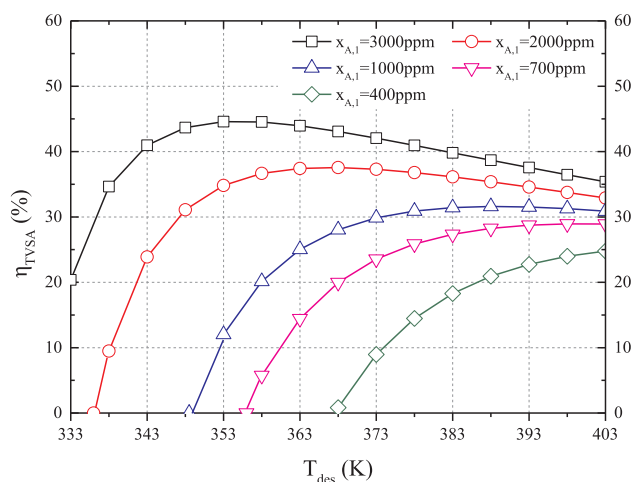

Fig. 5. The second-law efficiency of TVSA with different desorption temperatures and CO_2 levels in the feed gas at T_{ads} of 298 K.
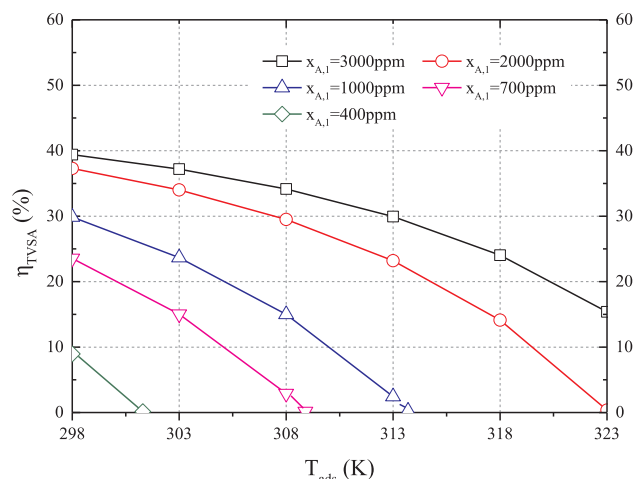
Fig. 6. The second-law efficiency of TVSA with different adsorption temperatures and CO_2 concentrations in the feed gas.
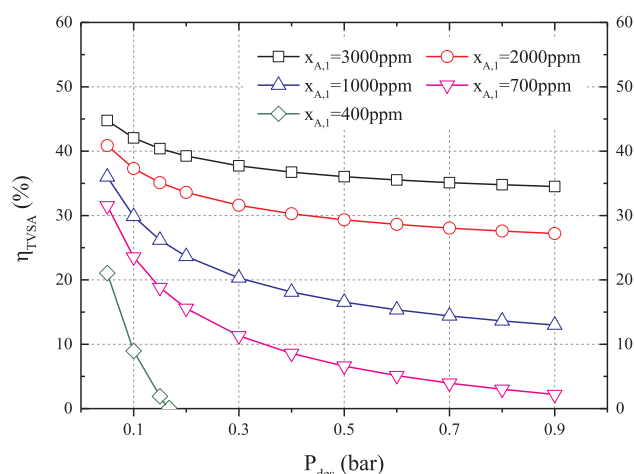

Fig. 7. The second-law efficiency of TVSA with various desorption pressures and CO_2 levels in the feed gas at T_{ads} of 298 K.

concerns about the existing studies of carbon emission reduction in the buildings are improving the efficiency of energy conversion and renewable energy utilization. As one of three critical technologies to reduce carbon emissions, CO_2 capture and storage (CCS) has received little attention in the building section.

What changes will be taken to buildings, especially the zero carbon buildings, with the application of the air ventilation system incorporating a DAC device? The answer will be the high energy consumption and a reduction of CO_2 in the air. Further discussions and conjectures will be provided in the following section.

4. Further exploration for approaching negative carbon buildings

The potential application of DAC in buildings, such as the air ventilation system incorporating direct air capture of CO_2, could make the zero carbon buildings further become approaching negative carbon buildings. Although there is a huge energy expenditure, the integrated air ventilation system brings major environmental benefits. On the one hand, DAC can reduce the indoor CO_2 levels by TVSA, which provides a high-level indoor air quality and consequent users' comfort. On the other hand, the applicable area of DAC is expanding into architecture such as office buildings and railway stations, which contribute to participate in carbon emission reduction activities for everyone. Therefore, DAC in buildings warrants attention in discussions as a potential win-win opportunity [21].
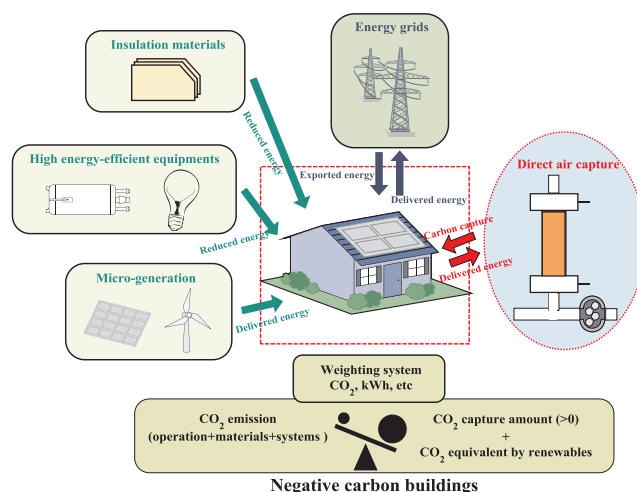

Fig. 8. System structure and basic elements for approaching negative carbon buildings.

4.1. Possibility and definition

The approach to achieve negative carbon buildings should be established on multi-aspect joint efforts, as shown in Fig. 8. Heat losses of buildings can be strongly reduced by using insulation materials. The high energy efficient equipment, such as low-energy lighting and heat pumps, should be installed in order to reduce energy demand and carbon emission [40]. The on-site micro-generation technologies, including solar, wind and hydro, are suitable for building installation with the generation of zero or low carbon heat and/or power to satisfy the energy requirement of buildings [41]. The application of DAC into buildings can solve the problems, including indoor air quality and direct carbon reduction, through smart grid connections and control. Generally, buildings consume delivered energy from energy grid, and export energy back to the grid as renewable technologies produce surplus electricity on site [42]. Therefore, the core principle for approaching negative carbon buildings is a weighting system which is chosen to calculate the net carbon emission reduction directly obtained by the whole system of buildings.

Actually, negative carbon buildings, as a dynamic concept, can be studied during varying periods in whole life cycle of the buildings. The common research methods, including experiment and simulation, can refer to the previous work of net-zero energy building [28]. Thus, negative carbon buildings in a scale of the whole life cycle should be defined as follows: negative carbon buildings are one where the carbon emission of the primary energy consumed in the building operation plus the carbon emission of the energy used in its constituent materials and systems, including energy generating ones, over the life of the building is less than the carbon emission equivalent of the energy produced by micro-generation technologies on site plus carbon capture amount by DAC technologies. However, it is important to note that carbon dioxide content outside the boundary of buildings is reduced substantially because of the existing DAC technologies, which is the obvious distinct point compared to zero carbon buildings.

4.2. Needs and challenges

It will complicate the existing air ventilation system for approaching negative carbon buildings. This integration scheme brings some changes and requirements, including good or bad ones. Specifically, the main solutions are explored as follows:

(1) *Power*: The air ventilation system incorporating a CO_2 capture device could increases aerodynamic drag, which may results in the increased power consumption of feed blowers when the flow rate is

maintained. However, this integration strategy can make full use of the ventilating pipes and fans of traditional air ventilation systems in buildings.

(2) *Cost*: The number of power components and the corresponding energy consumption will rise due to the addition of TVSA. The energy consumption of power components, such as vacuum pump and solenoid valves, can be supplied by micro-generation technologies including solar panels and wind systems, etc. This will result in the increased costs of the integrated ventilation system. However, the cost of a TVSA device for DAC could be approximately 200 USD/ton by the comprehensive consideration based on the studies of Brandani [12], Radosz et al. [43] and Keith et al. [44].

(3) *Energy saving and supply*: This method can flexibly change the air recirculation ratio according to the indoor and outdoor conditions so as to save air cooling or heating energy in buildings during hot summer or cold winter seasons [19]. The regeneration heat of adsorbent materials can be recovered by indoor air, which will provide a comfortable and warm environment during the heating season. Alternatively, the thermal energy for adsorbent regeneration can be supplied by solar thermal collectors on the roof of buildings.

(4) *Temperature*: The maximum desorption temperature of TVSA processes should be noticed and considered, which refers to the fire endurance of building materials that surround the adsorption chamber. In addition, the optimum desorption temperature of TVSA processes can be selected based on the second-law efficiency study.

(5) *Materials*: The adsorbent materials used for DAC should be harmless to the indoor environment with some suitable properties for CO_2 capture, such as selectivity and stability, etc. [8].

(6) *Control strategy*: Smarter control of a micro-grid with integrating a TVSA cycle for CO_2 capture, as an essential part of negative carbon buildings, can enable more dynamic energy flows about generation and consumption and more interaction between emission and capture. Thus, control strategies can become more flexible in different situations through a micro-grid [45]. In addition, if continuous run of the TVSA device is required, more columns of DAC could be designed to the alternate operation.

(7) *CO_2 sequestration*: Due to the requirement for approaching negative carbon buildings, the captured CO_2 can be explored for synthesis of value-added products with a minimal influence on climate change, such as methanol. The so-called power-to-x processes can make the excess electricity of micro-generation techniques convert to chemical energy.

5. Conclusion and future work

From the aspects of indoor comfort and environmental protection, the integrated strategy, which is the air ventilation system incorporating a TVSA device for DAC, has a great application value. A detailed thermodynamic analysis of the TVSA cycle is conducted and provided. The amine-functionalized cellulose, as a kind of chemosorbent, has been selected for the adsorbent material. The thermodynamic model of the TVSA cycle is evaluated in terms of minimum separation work and second-law efficiency. The results show the strong positive effects of CO_2 recovery, separation temperature and product purity on the minimum separation work for CO_2 capture processes. The minimum separation work of the cases of CO_2 level at 400 ppm is approximately 20 kJ/mol. In addition, the higher CO_2 feed levels, the larger second-law efficiencies of TVSA for DAC in buildings. The optimal second-law efficiencies are 44.57%, 37.55% and 31.60%, respectively for the cases of CO_2 level at 3000 ppm, 2000 ppm and 1000 ppm. The potential application of DAC in buildings, such as the cyclic operation of TVSA, may make the zero carbon buildings further upgrade to negative carbon buildings from a lifecycle viewpoint. Therefore, a life cycle carbon emission-energy-economic evaluation of the demonstrating building,

which contains the information of the whole life cycle for approaching negative carbon buildings, should be evaluated and testified in the near future.

Conflict of interest

The authors declared that there is no conflict of interest.

CRediT authorship contribution statement

Ruikai Zhao: Writing - original draft, Writing - review & editing, Visualization. **Longcheng Liu:** Supervision. **Li Zhao:** Funding acquisition, Project administration, Supervision. **Shuai Deng:** Conceptualization, Methodology, Data curation, Funding acquisition. **Shuangjun Li:** Data curation, Visualization. **Yue Zhang:** Data curation, Investigation. **Hailong Li:** Supervision.

Acknowledgements

References

[1] Warshaw C. Arctic sea ice at 1.5 and 2 °C. Nat Clim Change 2018;8:360–1.
[2] van Vuuren DP, Stehfest E, Gernaat DEHJ, van den Berg M, Bijl DL, de Boer HS, et al. Alternative pathways to the 1.5 °C target reduce the need for negative emission technologies. Nat Clim Change 2018;8:391–7.
[3] Jahn A. Reduced probability of ice-free summers for 1.5 °C compared to 2 °C warming. Nat Clim Change 2018;8:409–13.
[4] Scott V, Geden O. The challenge of carbon dioxide removal for EU policy-making. Nat Energy 2018;3:350–2.
[5] Möllersten K, Yan JR, Moreira J. Potential market niches for biomass energy with CO_2 capture and storage—opportunities for energy supply with negative CO_2 emissions. Biomass Bioenergy 2003;25:273–85.
[6] Dawid PH, Vasilije M. Combined heat and power generation with lime production for direct air capture. Energy Convers Manage 2018;160:455–66.
[7] Explainer: 10 ways 'negative emissions' could slow climate change; 2016. < https://www.carbonbrief.org/explainer-10-ways-negative-emissions-could-slow-climate-change > [accessed 11.28 2018].
[8] Wurzbacher JA, Gebald C, Steinfeld A. Separation of CO_2 from air by temperature-vacuum swing adsorption using diamine-functionalized silica gel. Energy Environ Sci 2011;4:3584–92.
[9] Li B, Duan Y, Luebke D, Morreale B. Advances in CO_2 capture technology: a patent review. Appl Energy 2013;102:1439–47.
[10] Mondal MK, Balsora HK, Varshney P. Progress and trends in CO_2 capture/separation technologies: a review. Energy 2012;46:431–41.
[11] Goeppert A, Czaun M, Surya Prakash GK, Olah GA. Air as the renewable carbon source of the future: an overview of CO_2 capture from the atmosphere. Energy Environ Sci 2012;5:7833–53.
[12] Brandani S. Carbon dioxide capture from air_ a simple analysis. Energy Environ 2012;23:319–28.
[13] Ounoughene G, Buskens E, Santos RM, Cizer Ö, Van Gerven T. Solvochemical carbonation of lime using ethanol: mechanism and enhancement for direct atmospheric CO_2 capture. J CO_2 Utiliz 2018;26:143–51.
[14] Wang T, Lackner KS, Wright A. Moisture swing sorbent for carbon dioxide capture from ambient air. Environ Sci Technol 2011;45:6670–5.
[15] Eisaman MD, Alvarado L, Larner D, Wang P, Garg B, Littau KA. CO_2 separation using bipolar membrane electrodialysis. Energy Environ Sci 2011;4:1319–28.
[16] Sanz-Perez ES, Murdock CR, Didas SA, Jones CW. Direct capture of CO_2 from ambient air. Chem Rev 2016;116:11840–76.
[17] Elfving J, Bajamundi C, Kauppinen J, Sainio T. Modelling of equilibrium working capacity of PSA, TSA and TVSA processes for CO_2 adsorption under direct air capture conditions. J CO_2 Utiliz 2017;22:270–7.
[18] Li Y, Yuan Y, Li C, Han X, Zhang X. Human responses to high air temperature, relative humidity and carbon dioxide concentration in underground refuge chamber. Build Environ 2018;131:53–62.
[19] Kim MK, Leibundgut H. Performance of novel ventilation strategy for capturing CO_2 with scheduled occupancy diversity and infiltration rate. Build Environ 2015;89:318–26.
[20] ANSI/ASHRAE. Standard 62.1-2013 ventilation for acceptable indoor air quality. Atlanta: American Society of Heating, Refrigerating and Air- Conditioning Engineers, Inc.; 2013.
[21] Gall ET, Nazaroff WW. New directions: Potential climate and productivity benefits

from CO_2 capture in commercial buildings. Atmos Environ 2015;103:378–80.

[22] Gall ET, Sonat C, Nazaroff WW, Unluer C. Investigating CO_2 removal by Ca- and Mg-based sorbents with application to indoor air treatment. Build Environ 2016;110:161–72.

[23] Kim MK, Baldini L, Leibundgut H, Wurzbacher JA, Piatkowski N. A novel ventilation strategy with CO_2 capture device and energy saving in buildings. Energy Build 2015;87:134–41.

[24] Lee TS, Cho JH, Chi SH. Carbon dioxide removal using carbon monolith as electric swing adsorption to improve indoor air quality. Build Environ 2015;92:209–21.

[25] Han GB, Jang JH, Lee TJ, Choi C. Performance test of PSA-type O_2 separator for efficient O_2 supply to room ventilation system combined with CO2 adsorption module. Korean J Chem Eng 2016;33:1311–7.

[26] Hu S-C, Shiue A, Chang S-M, Chang Y-T, Tseng C-H, Mao C-C, et al. Removal of carbon dioxide in the indoor environment with sorption-type air filters. Int J Low-Carbon Technol 2017;12:330–4.

[27] Xing Y, Hewitt N, Griffiths P. Zero carbon buildings refurbishment—a Hierarchical pathway. Renew Sustain Energy Rev 2011;15:3229–36.

[28] Deng S, Wang RZ, Dai YJ. How to evaluate performance of net zero energy building – a literature research. Energy 2014;71:1–16.

[29] Su F, Lu C. CO_2 capture from gas stream by zeolite 13X using a dual-column temperature/vacuum swing adsorption. Energy Environ Sci 2012;5(10):9021–7.

[30] Plaza MG, García S, Rubiera F, Pis JJ, Pevida C. Post-combustion CO_2 capture with a commercial activated carbon: comparison of different regeneration strategies. Chem Eng J 2010;163:41–7.

[31] Gebald C, Wurzbacher JA, Borgschulte A, Zimmermann T, Steinfeld A. Single-component and binary CO_2 and H_2O adsorption of amine-functionalized cellulose. Environ Sci Technol 2014;48:2497–504.

[32] Wurzbacher JA, Gebald C, Brunner S, Steinfeld A. Heat and mass transfer of temperature–vacuum swing desorption for CO_2 capture from air. Chem Eng J 2016;283:1329–38.

[33] Zhao R, Zhao L, Deng S, Song C, He J, Shao Y, et al. A comparative study on CO_2 capture performance of vacuum-pressure swing adsorption and pressure-temperature swing adsorption based on carbon pump cycle. Energy 2017;137:495–509.

[34] Zhao R, Deng S, Wang S, Zhao L, Zhang Y, Liu B, et al. Thermodynamic research of adsorbent materials on energy efficiency of vacuum-pressure swing adsorption cycle for CO_2 capture. Appl Therm Eng 2018;128:818–29.

[35] Lively RP, Realff MJ. On thermodynamic separation efficiency: adsorption processes. AIChE J 2016;62:3699–705.

[36] Zhao R, Deng S, Liu Y, Zhao Q, He J, Zhao L. Carbon pump: fundamental theory and applications. Energy 2017;119:1131–43.

[37] Jiang L, Roskilly AP, Wang RZ. Performance exploration of temperature swing adsorption technology for carbon dioxide capture. Energy Convers Manage 2018;165:396–404.

[38] Zhao R, Deng S, Zhao L, Zhao Y, Li S, Zhang Y, et al. Experimental study and energy-efficiency evaluation of a 4-step pressure vacuum swing adsorption (PVSA) for CO_2 capture. Energy Convers Manage 2017;151:179–89.

[39] Lackner KS. The thermodynamics of direct air capture of carbon dioxide. Energy 2013;50:38–46.

[40] Jiang L, Roskilly AP, Wang RZ, Wang LW. Analysis on innovative resorption cycle for power and refrigeration cogeneration. Appl Energy 2018;218:10–21.

[41] Jiang L, Lu YJ, Roskilly AP, Wang RZ, Wang LW, Tang K. Exploration of ammonia resorption cycle for power generation by using novel composite sorbent. Appl Energy 2018;215:457–67.

[42] Yang G, Zhai X. Optimization and performance analysis of solar hybrid CCHP systems under different operation strategies. Appl Therm Eng 2018;133:327–40.

[43] Radosz M, Hu X, Krutkramelis K, Shen Y. Flue-gas carbon capture on carbonaceous sorbents: toward a low-cost multifunctional carbon filter for "green" energy producers. Ind Eng Chem Res 2008;47:3783–94.

[44] Keith DW, Holmes G, St. Angelo D, Heidel K. A Process for Capturing CO_2 from the Atmosphere. Joule 2018;2:1573–94.

[45] Zhang Y, Deng S, Zhao L, Lin S, Ni J, Ma M, et al. Optimization and multi-time scale modeling of pilot solar driven polygeneration system based on organic Rankine cycle. Appl Energy 2018;222:396–409.